

Trojan Cleansing with Neural Collapse

Xihe Gu

University of California, San Diego
9500 Gilman Dr, La Jolla, CA 92093

x9gu@ucsd.edu

Tara Javidi

tjavidi@ucsd.edu

Greg Fields

grfields@ucsd.edu

Yaman Jandali

yeljanda@ucsd.edu

Farinaz Koushanfar

fkoushanfar@ucsd.edu

Abstract

Trojan attacks are sophisticated training-time attacks on neural networks that embed backdoor triggers which force the network to produce a specific output on any input which includes the trigger. With the increasing relevance of deep networks which are too large to train with personal resources and which are trained on data too large to thoroughly audit, these training-time attacks pose a significant risk. In this work, we connect trojan attacks to Neural Collapse, a phenomenon wherein the final feature representations of over-parameterized neural networks converge to a simple geometric structure. We provide experimental evidence that trojan attacks disrupt this convergence for a variety of datasets and architectures. We then use this disruption to design a lightweight, broadly generalizable mechanism for cleansing trojan attacks from a wide variety of different network architectures and experimentally demonstrate its efficacy.

1. Introduction

Over the past decade, deep neural networks have achieved state-of-the-art performance in a vast array of sensitive machine learning (ML) tasks such as autonomous driving, medical diagnostics, and financial portfolio management. The unprecedented speed of this adoption, along with prior research establishing the vulnerability of these methods to a wide variety of attacks, has made the study of security and safety of ML models an important area of research. This paper considers an important class of training-time attacks on these models known as trojan attacks.

Trojan attacks, or backdoor attacks, aim to maliciously corrupt a neural network’s training process such that the presence of a *trojan trigger* in any input will force the network to produce a target classification [10]. This type of attack is generally accomplished by means of *data poisoning*, where the adversary adds their chosen trigger to a small

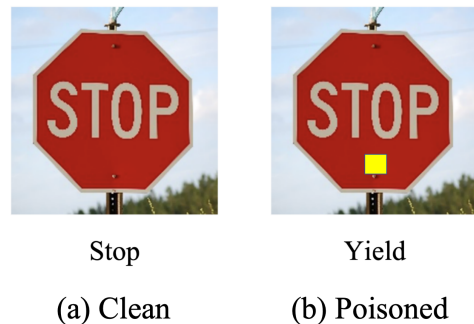


Figure 1. An example of trojan attack on a traffic sign classifier. (a) model works normally on clean data without triggers, (b) attackers manipulate the prediction by adding a specific trigger. Image due to [27].

portion of a training dataset and labels the poisoned samples with their selected target class. Models trained on this dataset then learn both the correct classifications for clean data and the malicious classification for inputs containing the trigger. Fig. 1, provided in [27], illustrates an example of clean data point (a) along a poisoned one (b). The yellow trigger in this example is clearly visible, but [25] showed that poisoning may take on a subtle nature that is undetectable by human auditors so that that malicious behavior can be hidden until test time or model deployment.

In this paper, for the first time, we make a concrete connection between training with poisoned data and a phenomenon recently studied in the deep learning theory literature, called Neural Collapse [24]. Neural Collapse describes the widely observed phenomenon wherein, over the course of training a neural network, highly symmetric structures emerge in both the network’s weights and the feature representations of training samples. In contrast, trojan attacks are inherently asymmetric: they require *any input* be classified to a single target class given only the presence of a small perturbation. We hypothesize and experimentally demonstrate that the injection of a trojan trigger into a

neural network breaks the symmetries of Neural Collapse. We then use these results to develop a carefully targeted, lightweight method for mitigating trojan attacks that is both architecture and dataset agnostic.

1.1. Contributions

There is a large body of work on trojan detection and mitigation, detailed in Sec. 2.2. Some of these approaches first attempt to understand how trojan triggers alter the structure of neural networks: Neural Cleanse [29] suggests that triggers activate a certain subset of neurons, the topological analysis of [35] finds that triggers introduce an unusual number of skip connections between early and late layers in the network. But these analyses are generally unable to predict precisely where and how a trigger will manifest in a particular neural network and must rely on data-driven approaches to identify, for instance, the particular subset of neurons which comprise the action of the trigger.

We pursue this question through the inherent asymmetry introduced by training on poisoned datasets and the natural impact this has on the Neural Collapse (NC) phenomenon. We discuss NC in depth in Sec. 2.3, but, briefly, NC is a feature of training over-parameterized models where, as shown in Fig. 2, the final feature representations of the training data and the weight matrix of the final layer of the network, both, converge to a simple and highly symmetric geometric structure. We hypothesize that this symmetric structure, however, directly contradicts the asymmetry introduced by data poisoning. In this work, we present extensive experimental evidence supporting this hypothesis and show that the process of embedding a trojan in a neural network significantly weakens the NC phenomenon in measurable and predictive ways.

We leverage these insights to initiate a new class of trojan *cleansing* methods: algorithms which take a potentially trojaned network and by imposing NC-inspired symmetry remove the trojan trigger while maintaining the network’s performance on clean data. In other words, identifying the predictive impact the trojan embedding has on NC metrics allows us to arrive at an entirely new method for cleansing. Many existing cleansing methods, as detailed in Sec. 2.2, rely either on some form of model compression, which may harm the model’s generalization capabilities, or on reconstructing the trojan trigger, which relies on knowledge of the class of the triggers the adversary may have chosen from. In contrast, we are able to introduce a small and carefully targeted adjustment to a small subset of the weights of the network without any knowledge of the possible trojan triggers: mitigating the attack without deteriorating the generalization power of the model.

We conduct extensive evaluations of our cleansing method, comparing with many other standard cleansing algorithms over different network architectures and types of

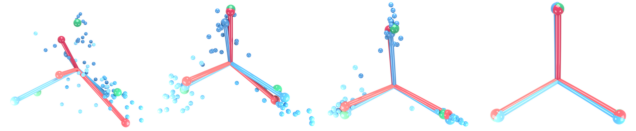


Figure 2. The figure illustrates NC as training progresses from left to right. Green spheres represent the vertices of an ETF, red points represent the linear classifiers, large blue/green points represent class means, and small blue/green points represent final layer features, with different shades indicating different classes. As training progresses, the features concentrate. Figure due to [24].

trojan attacks. Our experiments show that our cleansed network effectively maintains the accuracy of the original network on unseen, un-triggered test data, but is no longer susceptible to the trojan trigger. We achieve comparable performance to other cleansing algorithms against standard data poisoning attacks on ResNet architectures and state-of-the-art performance against more sophisticated trojan attacks and large transformer architectures. Additional experiments show our algorithm is particularly robust to data imbalance and corruption. Moreover, our algorithm is very lightweight and easy to implement for any standard classification network architecture. This stands in contrast to many other common cleansing techniques and is particularly important since the trojan threat model assumes that the user must outsource their model training and so likely has limited ML resources and expertise.

2. Related Work

2.1. Trojan Attacks

The baseline data poisoning trojan attack was explored in [5] and [10]. The TrojanNN [19] attack, on a pre-trained model, carefully designs a trigger via network analysis and then reinforces it with a data poisoning step. Wanet [23] introduces warping-based triggers, while ReFool [20] introduces reflection triggers, both offering stealthier triggers than traditional trojan attacks. Instead of using the manually defined trigger, Lira [8] jointly learns a subtle trigger injection function while poisoning the model.

Our work in this paper focuses on the image domain, but trojans have also been proven effective in other domains: [6] and [7] implement trojan attacks on language data and [32] poisons audio data to trojan a model for speech recognition. Extending our analysis and cleansing mechanism to these domains is an interesting direction for future work.

2.2. Model Cleansing

Li et al. [17] and Xia et al. [31] use forms of distillation to preserve only the model’s performance on clean data while Wang et al. [29] identifies and prunes neurons likely associated with the trojan trigger. Other approaches rely on first

reconstructing potential triggers and then attempt to remove them: [4] learns a generative model to create likely triggers and then corrects the network via adversarial training. Zeng et al. [33] proposes a minimax formulation and computationally efficient optimization scheme for trigger reconstruction. Other approaches include [15], which leverages sparse reconstruction of inputs and feature representations to remove potential triggers, and [37], which applies adversarial training to a new layer inserted into the network. [36] is a detection and mitigation method that shrinks the norms of backdoor-related neurons by using sharpness-aware minimization with fine-tuning. Wu et al. [30] introduced BackdoorBench, a platform which implements many of these algorithms and provides a leader board that guides our benchmark selection in Sec. 4.2.

We note that our work is related but fundamentally distinct from trojan detection which aims to determine whether a model may be trojaned, including those focusd on data analysis, as in Baracaldo et al. [2], Liu et al. [18], Shen et al. [26] as well as those work that directly analyze the model, such as Chen et al. [3], Fields et al. [9], Ma et al. [21].

2.3. Neural Collapse

Neural Collapse is a phenomenon, first reported by Papayan et al. [24] and thoroughly reviewed by [16], which has been observed across a wide variety datasets and model architectures. It describes a process observed in over-parameterized classification deep neural networks which are trained past zero training error, into a period referred to as the terminal phase of training (TPT). As depicted in Fig. 2, as the TPT progresses, the final feature representations of the training data and the weight matrix of the network’s last layer converge to a highly uniform, symmetric geometric structure known as a simplex equiangular tight frame (simplex ETF).

While NC is associated with models trained past perfect training accuracy, this practice is known to have practical benefits as in the double descent phenomenon [22]. Further experiments in [24] demonstrate in particular that the TPT offers advantages including improved generalization performance, enhanced robustness, and increased interpretability. Various theoretical models, based on locally elastic dynamics [34] and unconstrained features [37, 38] have begun examining how NC arises and its connections to these other neural network characteristics.

It is important to note that Neural Collapse is not a binary phenomenon that either does or does not occur. In practice the characteristics of collapse arise even before the TPT and gradually converge over the course of the TPT. Consequently, our discussion of NC will focus on its degree, quantified by four metrics which converge to zero as the qualitative characteristics of NC obtain. We will define these metrics in Sec. 3.2 after introducing notation.

3. Neural Collapse Disruption Hypothesis

[24] and [12] observed and proposed metrics for Neural Collapse across diverse architectures and datasets. In this section, we review these metrics, and provide evidence that trojan triggers weaken Neural Collapse phenomenon. In particular, we evaluate various NC metrics associated with a variety of trojaned models and show that every trojaned model has at least one weaker NC metric. Furthermore, benign models consistently achieve at least the same degree of collapse as their trojaned counterparts across all metrics.

3.1. Neural Collapse: Definitions

We consider a deep learning classification problem with K classes, d -dimensional training samples $\mathbf{X}_i = \{x_1, \dots, x_{n_i}\}$ for each class i , and neural network $f: \mathbb{R}^d \rightarrow \mathbb{R}^K$. Our analysis will focus on the final feature representation of the network, so we will decompose the network as $f(\mathbf{x}) = \mathbf{W}g(\mathbf{x}) + \mathbf{b}$, with $\mathbf{W} \in \mathbb{R}^{K \times m}$ and $\mathbf{b} \in \mathbb{R}^m$ giving the final fully-connected layer’s weights and biases, and $g: \mathbb{R}^d \rightarrow \mathbb{R}^m$ calculating the network’s final m -dimensional feature representation.

The trojan attacks we evaluate in our experiments are carried out via data poisoning. To implement such an attack, we first choose a trigger function $\kappa: \mathbb{R}^d \rightarrow \mathbb{R}^d$. In our experiments this function will be the overlay of a small, solid patch on the base image, as shown in Fig. 1, or the application of an Instagram filter to the base image, as shown in Fig. 7. We then choose a poisoning proportion $\delta \in [0, 1)$ and a target class $k_T \in [K]$. For each \mathbf{X}_k with $k \neq k_T$ and each sample $\mathbf{x} \in \mathbf{X}_k$, with probability δ we delete \mathbf{x} from \mathbf{X}_k and add $\kappa(\mathbf{x})$ to \mathbf{X}_{k_T} . We say a model is *trojaned* if $\delta > 0$, and a model is *benign* if $\delta = 0$.

The Neural Collapse phenomenon is observed primarily in two sets of values. The first are the rows of the final layer weights associated with each class, given by $\mathbf{W} = [\mathbf{w}_1, \dots, \mathbf{w}_K]^T$, where each row $\mathbf{w}_k \in \mathbb{R}^m$ gives the weights of the final classifier layer associated with class k . The second are the centered class means of the final feature representations of the training samples. Define the feature means and the global feature mean:

$$\boldsymbol{\mu}_k := \frac{1}{|\mathbf{X}_k|} \sum_{\mathbf{x} \in \mathbf{X}_k} g(\mathbf{x}), \quad \boldsymbol{\mu}_G := \frac{1}{K} \sum_{k=1}^K \boldsymbol{\mu}_k.$$

Then we can construct the matrix of centered feature means, $\mathbf{M} := [\boldsymbol{\mu}_1 - \boldsymbol{\mu}_G, \dots, \boldsymbol{\mu}_K - \boldsymbol{\mu}_G]^T =: [\mathbf{m}_1, \dots, \mathbf{m}_K]^T$, and quantify the degree of Neural Collapse in terms of a variety of characteristics of the \mathbf{M} and \mathbf{W} matrices.

3.2. Neural Collapse: Metrics and Trojan Impact

The observed phenomenon of Neural Collapse can be more precisely described by a set of four characteristics laid out in [24] and quantified by a standard set of metrics defined in [12] and used in other analyses of NC such as [11] and [14]. In this section we will describe these metrics and

present results comparing their convergence over the course of training for both benign and trojaned models on CIFAR-10, CIFAR-100, and GTSRB datasets. Our results show that the application of a trojan trigger causes the NC metrics to converge more slowly and to a larger value than their benign counterparts. There is variation in this behavior across different datasets and different metrics, but in every case the trojaned model shows weaker collapse.

NC1: Variability collapse The final feature representation of every training sample in every class converges to the mean of the feature representations of the samples from their respective classes. Equivalently, the variability of feature representations within any given class vanishes. This can be quantified by defining the within-class and between-class covariances

$$\Sigma_W := \frac{1}{K} \sum_{k=1}^K \frac{1}{|\mathbf{X}_k|} \sum_{\mathbf{x} \in \mathbf{X}_k} \left((g(\mathbf{x}) - \boldsymbol{\mu}_k)(g(\mathbf{x}) - \boldsymbol{\mu}_k)^T \right)$$

$$\Sigma_B := \frac{1}{K} \sum_{k=1}^K \mathbf{m}_k \mathbf{m}_k^T.$$

The degree of variability collapse is then quantified by the relationship between the spread of features within a class relative to the spread between the feature means of different classes:

$$\text{NC1} := \frac{1}{K} \text{tr}\{\Sigma_W \Sigma_B^T\}. \quad (1)$$

Experimental evaluation of NC1 for both benign and trojaned models are shown in Fig. 3 and Tab. 1. On CIFAR-10 we did not observe a significant difference between the benign and trojaned models for this metric, but convergence of NC1 was significantly weaker in our experiments on CIFAR-100 and GTSRB. Note that the red dashed line in all figures represents the point at which the models achieve zero training error, and so the beginning of the terminal phase of training.

NC2: Convergence to a simplex ETF Both \mathbf{M} and \mathbf{W} converge to a simplex ETF. In particular, this means that

the norms of each of the rows equalize and that they become maximally pairwise separated from each other as measured by cosine similarity. Note that the maximum pairwise cosine similarity among a set of K vectors is $(1-K)^{-1}$. These two characteristics can be quantified, respectively, by the two statistics

$$\text{NC2}_{\text{Norm}}(\mathbf{V}) := \frac{\text{std}_{k \in [K]}(\|\mathbf{v}_k\|_2)}{\text{mean}_{k \in [K]}(\|\mathbf{v}_k\|_2)} \quad (2)$$

$$\text{NC2}_{\text{Angle}}(\mathbf{V}) := \text{mean}_{i,j \in [K], i < j} \left(\cos(\mathbf{v}_i, \mathbf{v}_j) + \frac{1}{K-1} \right).$$

Fig. 6 tracks Eq. (2), which characterizes the convergence of both the classifier weights, \mathbf{W} and the centered class means, \mathbf{M} to a simplex ETF. For the equinorm property, shown in Fig. 6a, the benign model shows the most uniformity in norm across both feature means and classifier weights, and as the percentage of trojaned data increases, the equinorm property weakens. This trend is particularly profound in the classifier weights. We note that, for both class means and classifiers, this is caused by the fact that the norm of the target class is consistently *smaller* than those of other classes. For the equiangular property a similar, though smaller trend is observed.

NC3: Convergence to self-duality The rows of the final layer weight matrix \mathbf{W} converge to a simplex ETF dual to that of the feature representations. Given NC2, this means that \mathbf{W} and \mathbf{M} converge, up to a rescaling by their respective Frobenius norms.

$$\text{NC3} := \left\| \frac{\mathbf{W}}{\|\mathbf{W}\|_F} - \frac{\mathbf{M}}{\|\mathbf{M}\|_F} \right\|^2 \quad (3)$$

Fig. 4 shows this metric also converges to a smaller value for the benign model than either trojaned model and the disruption to Neural Collapse increases with the proportion of training data poisoned.

NC4: Nearest feature mean classification At inference time, the neural network uses a nearest neighbor decision

	CIFAR-100			GTSRB			
	Benign	1%	5%	Benign	5%	10%	20%
NC1	0.8917	0.9165	0.8830	0.1567	1.3484	2.2541	5.0615
NC2 _{Norm} (\mathbf{M})	0.0325	0.0372	0.0453	0.1679	0.1666	0.1905	0.1775
NC2 _{Norm} (\mathbf{W})	0.0089	0.0169	0.0527	0.1796	0.2166	0.2584	0.2798
NC2 _{Angle} (\mathbf{M})	0.0511	0.0507	0.0513	0.0719	0.0862	0.0777	0.0952
NC2 _{Angle} (\mathbf{W})	0.0518	0.0513	0.0520	0.0625	0.0778	0.0651	0.0988
NC3	0.0174	0.0183	0.0254	0.1419	0.1747	0.2115	0.2376
NC4	0.0000	0.0000	0.0001	0.0000	0.0174	0.0691	0.1680

Table 1. Comparison of all NC metrics between trojaned and benign models for CIFAR-100 and GTSRB. \mathbf{M} refers to the matrix of class means of the final-layer feature representations; \mathbf{W} denotes the weight matrix of the final fully-connected layer. The percentage indicates the poison rate for the training dataset of the trojaned models.

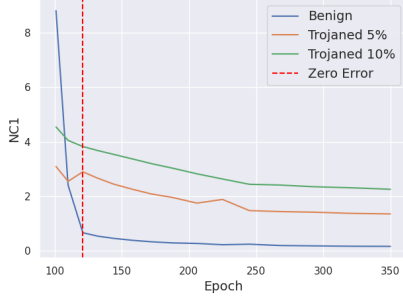


Figure 3. **Variability Collapse** Comparison of the convergence of trojaned and benign models on the NC1 metric [Eq. (1)] for GT-SRB on ResNet18.

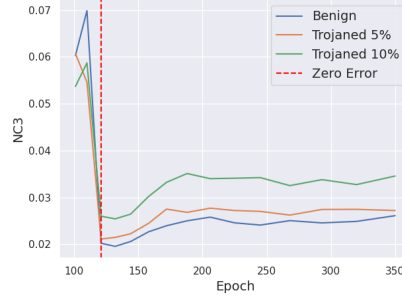


Figure 4. **Self-duality** Comparison of the convergence of trojaned and benign models on the NC3 metric [Eq. (3)] for CIFAR-10 on ResNet18.

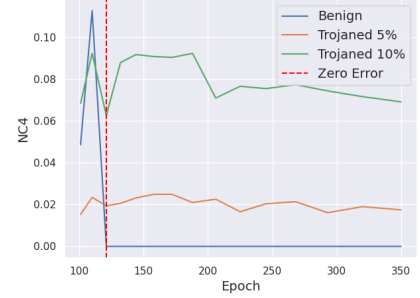
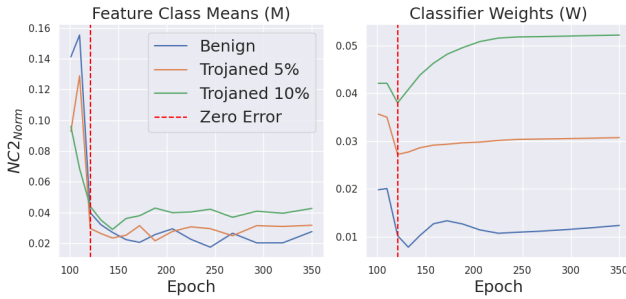
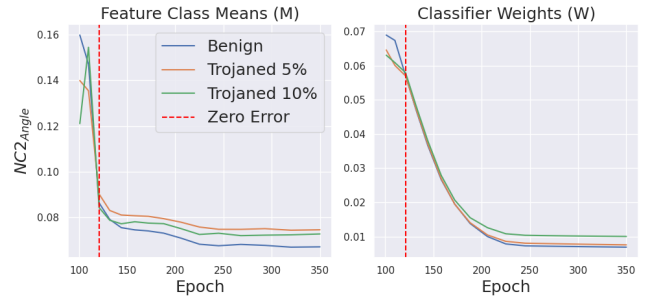


Figure 5. **Nearest feature classification** Comparison of the convergence of trojaned and benign models on the NC4 metric [Eq. (4)] for GTSRB on ResNet18.



(a) **Equinorm** metric [Eq. (2)] for the feature class means and the final classifier layer weight matrix.



(b) **Equiangular** metric [Eq. (2)] for the feature class means and the final classifier layer weight matrix.

Figure 6. **Convergence to ETF** Comparison of the convergence of trojaned and benign models on the NC2 metrics for CIFAR-10 on ResNet18.

rule in the final feature space. That is, a new test point is classified to the class with the feature mean nearest to its own feature representation. A metric for this is then the misclassification rate for this decision rule.

$$\text{NC4} := \frac{1}{K} \sum_{k=1}^K \frac{1}{|\mathbf{X}_k|} \sum_{\mathbf{x} \in \mathbf{X}_k} \mathbb{I} \left(\arg \max_{c \in [K]} \mathbf{w}_c^T g(\mathbf{x}) + b_c \neq \arg \min_{c \in [K]} \|g(\mathbf{x}) - \boldsymbol{\mu}_c\|_2 \right) \quad (4)$$

Similar to NC1, on CIFAR-10 we did not observe a significant difference between the benign and trojaned models for NC4 as the nearest neighbor rule reaches perfect accuracy for each of them. But collapse is noticeably weakened in this metric in our experiments on CIFAR-100 and GTSRB, as shown in Fig. 5 and Tab. 1.

4. Trojan Cleansing Method (ETF-FT)

4.1. Methodology

This tension motivates an algorithm for cleansing a network of any potential trojan triggers, which we name **ETF-FT**. ETF-FT aims to take a fully trained, possibly trojaned

neural network and remove trojan triggers, if any exist, while maintaining the network’s good performance on clean test data. The effects of a trojan attack are most apparent in Fig. 6a, which shows that the weights of the final layer of a benign neural network exhibit a much greater degree of symmetry than those of an analogous trojaned network. So, as specified in Algorithm 1, we proceed by first overwriting the weights of the final fully-connected layer to a randomly generated simplex ETF, freezing those weights, and then fine-tuning the remaining model parameters on a small subset of clean data. Notably, this process works robustly with limited data, and the fine-tuning data does not necessarily need to come from the original training set.

Algorithm 1 Trojan Cleansing with Neural Collapse (ETF-FT)

Input: Trojanged model h_{troj} , clean dataset $\mathbf{X}_{\text{clean}}$

Step 1: Replace weight matrix with \mathbf{W}_{ETF}

Construct random ETF \mathbf{W}_{ETF}

Replace the final layer weight matrix with \mathbf{W}_{ETF}

Step 2: Fine-tune the model

Freeze the final layer weight matrix

Fine-tune on the clean dataset $\mathbf{X}_{\text{clean}}$

Output: Cleansed model h_{cleansed}

ETF-FT is motivated by our results which show that trojans work, in part, by deforming the symmetric structure NC describes in the weights of the final layer. By fixing those weights to be a random, but perfectly symmetric ETF our algorithm accomplishes two things: first, it prevents the trojan deformation of the final layer and second, it resets the weights in a way known to be compatible with good classification. This addresses a challenge present in many trojan cleansing techniques: the more you perturb the poisoned model the less effective the trigger will be, but the harder is it to recover accuracy on clean data.

4.2. Experiment Details

We compare our method with a variety of state-of-the-art cleansing algorithms that have demonstrated strong performance on the BackdoorBench [30] leaderboard. As a baseline, we also run vanilla fine-tuning, with no trojan-aware modifications, on the same subset of clean data—these results are labeled FT in the following tables. Our evaluation considers two types of backdoor attacks: BadNets-A2O [10] and TrojanNN [19], and two model architectures: PreAct-ResNet18 [13] and ViT-B/16 [1].

We focus on two key metrics to evaluate the performance of each cleansing method: accuracy on clean data (ACC) and attack success rate (ASR). Accuracy reflects the model’s performance on clean data after cleansing, ide-

ally showing no reduction compared to the original model. ASR, on the other hand, measures the proportion of poisoned samples classified as the attack target class. An effective cleansing method should reduce ASR to nearly zero.

We utilize the BackdoorBench repository [30] implementations of all attacks and cleansing methods besides our own. For experiments on PreAct-ResNet18, we use the original hyperparameters provided in the repository. By default, the repository uses 5% of the training data as available clean data for fine-tuning, though we also run experiments with 1% of training data and with imbalanced and corrupted data, as in real world situations the end user may not have access to (much of) the original training data.

We also evaluate the cleansing algorithm’s performance on a vision transformer, due to the popularity and efficacy of transformer architectures. However, many cleansing algorithms are not designed with transformers in mind. We adapted algorithms to the new architecture where necessary, as in NPD, which inserts a new layer into the network, we chose to insert a linear layer before the final layer of the transformer encoder. We also did light hyperparameter tuning over batch size, learning rate, scheduler and decay rate for each algorithm including our own. Despite this, many algorithms show poor performance in this setting relative to their results on ResNet. Many of these algorithms may be capable of better performance on transformers given careful adaptation, but in the trojan attack scenario the end user has outsourced network training to an adversary and so is unlikely to be a sophisticated deep learning engineer. As such, it is a significant strength of our algorithm that it can be applied to any classifier architecture without modification.

4.3. Results

BadNet Attack Tab. 2 presents the cleansing results for the BadNet attack. When the cleansing algorithms are allowed to use 5% of the training data to fine-tune, on the ResNet model, ETF-FT achieves competitive ASR while maintaining high accuracy on clean data relative to the other meth-

Method	PreAct-ResNet18[13]				ViT-B/16[1]			
	5% Clean data		1% Clean data		5%		1%	
	ACC	ASR	ACC	ASR	ACC	ASR	ACC	ASR
Original	88.95	95.06	88.95	95.06	95.43	87.06	95.43	87.06
FT	91.63 ± 0.18	10.03 ± 7.23	90.20 ± 0.22	22.04 ± 25.38	96.06	20.46	95.74	36.87
NCleanse[29]	91.57 ± 0.1	0.98 ± 0.12	89.90 ± 0.34	1.12 ± 0.18	96.08	0.28	95.61	2.70
NAD[17]	91.30 ± 0.18	2.20 ± 0.43	88.88 ± 0.28	10.19 ± 12.98	94.25	2.12	95.24	29.42
NPD[37]	85.71 ± 3.59	3.39 ± 2.47	83.26 ± 3.59	5.26 ± 3.82	91.38	50.35	91.92	85.17
FT-SAM[36]	92.23 ± 0.12	2.37 ± 0.81	90.33 ± 0.15	8.12 ± 11.86	96.38	1.93	94.29	6.16
I-BAU[33]	88.78 ± 1.53	5.53 ± 6.81	86.16 ± 0.91	32.79 ± 18.81	25.96	10.87	12.91	68.68
ETF-FT(ours)	91.77 ± 0.16	2.85 ± 0.68	90.24 ± 0.28	4.22 ± 2.05	91.99	1.15	87.55	1.60

Table 2. Comparison of cleansing algorithms on trojanged models trained on 10% poisoned data with the **BadNet** attack. Results are reported on CIFAR-10. Results on ResNet18 are averaged over 10 random trials with mean±std; result on ViT is a single trial.

Method	PreAct-ResNet18[13]				ViT-B/16[1]			
	5% Clean data		1% Clean data		5%		1%	
	ACC	ASR	ACC	ASR	ACC	ASR	ACC	ASR
Original	91.17	99.90	91.17	99.90	96.67	100.00	96.67	100.00
FT	91.92 ± 0.15	3.12 ± 3.14	90.60 ± 0.37	3.75 ± 6.41	95.94	100.00	95.98	100.00
NCleanse[29]	91.49 ± 0.45	41.07 ± 48.04	90.50 ± 1.05	70.67 ± 44.64	96.80	2.33	96.52	40.96
NAD[17]	91.36 ± 0.28	1.51 ± 0.37	88.39 ± 0.89	2.99 ± 1.94	89.99	100.00	96.40	100.00
NPD[37]	82.65 ± 2.14	16.34 ± 11.34	86.87 ± 0.13	43.03 ± 1.68	96.69	100.00	96.50	100.00
FT-SAM[36]	90.78 ± 0.21	8.10 ± 4.62	87.52 ± 0.60	12.23 ± 19.80	96.98	100.00	96.82	100.00
I-BAU[33]	91.83 ± 0.12	82.22 ± 1.73	91.73 ± 0.25	99.91 ± 0.01	36.10	9.74	36.70	0.41
ETF-FT(ours)	92.39 ± 0.24	0.04 ± 0.05	91.01 ± 0.47	0.00 ± 0.00	95.34	10.76	95.04	10.11

Table 3. Comparison of cleansing algorithms on trojaned models trained with 10% poisoned data with the **TrojanNN** attack. Results are reported on CIFAR-10. Results on ResNet are averaged over 10 random trials with mean±std; result on ViT is a single trial.

ods tested. In more restrictive conditions, where only 1% of the training data is available, ETF-FT and Neural Cleanse maintain strong performance, while other methods show significant degradation. The numbers in red indicate extremely poor performance, failing to function as an effective cleansing method.

Vision Transformers Despite their state-of-the-art performance and growing popularity, vision transformers have rarely been examined in the context of backdoor cleansing performance. This is in part due to the fact that their distinct architecture makes it difficult to adapt many common cleansing methods. Tab. 2 shows cleansing results for the BadNet attack applied to the ViT model, ETF-FT achieves very low ASR in both standard and limited data conditions, surpassing other methods except Neural Cleanse in the standard data case. This does come at the cost of a trade-off with in clean accuracy, which we believe can be mitigated, as discussed in Sec. 5.1.

TrojanNN Attack Alongside the standard BadNet attack, we consider the more sophisticated TrojanNN attack [19] which identifies specific vulnerable neurons in a pre-trained network and reverse engineers a subtle trigger to target them. As shown in Tab. 3, ETF-FT is particularly well suited to cleansing this style of trojan. On ResNets, ETF-FT completely eliminates the trigger, achieving an ASR of nearly 0 across 10 trials, while maintaining competitive accuracy with the other cleansing methods. On ViT, many methods, implemented out of the box, fail completely to eliminate the trigger, while ETF-FT achieves an ASR of 10% with only a 1.5 point drop in clean accuracy. I-BAU algorithm is able to almost entirely eliminate the trigger, but in doing so destroyed the model’s accuracy on clean data.

4.3.1. Robustness

The above results show that ETF-FT performs well with access to only a small amount of training data. But it is likely that the user of a trojaned model may not have access to any data from the original training distribution at all. We sim-

ulated distribution shift in two ways: by imbalancing the class distribution and by applying random erasures within image patches. Results for these datasets, applied to the ResNet BadNet poisoned models, are shown in Tab. 4 and Tab. 8 (in Appendix A). In both settings, ETF-FT excels at maintaining the model’s clean accuracy along with competitive ASR relative to other methods. Neural Cleanse, which had generally very strong results in this setting with training data, performs significantly better than all other methods on the imbalanced data, but its clean accuracy suffers on the corrupted data. This is due to the fact that its pruning method relies on identifying important neurons based on their activations on the available data—so it is vulnerable to accidentally pruning neurons associated with valid features which aren’t represented in the fine-tuning dataset.

Method	ACC	ASR
Original	88.95	95.06
FT	81.66 ± 0.39	1.76 ± 0.48
NCleanse[29]	81.80 ± 0.38	1.72 ± 0.38
NAD[17]	67.14 ± 1.96	3.10 ± 1.68
NPD[37]	83.10 ± 3.64	5.97 ± 4.59
FT-SAM[36]	85.23 ± 0.77	1.21 ± 0.48
I-BAU[33]	86.65 ± 1.38	28.26 ± 17.91
ETF-FT(ours)	87.99 ± 0.49	3.37 ± 2.80

Table 4. **Data Corruption:** Comparison of cleansing algorithms with 1% corrupted (under random erasure) clean training data on BadNet trojaned models. Results are reported on 10% Badnets trojaned CIFAR-10 using PreAct-ResNet18, averaged over 5 random trials with mean±std.

4.3.2. More Sophisticated Trigger

To thoroughly evaluate the performance of ETF-FT against Trojan attacks with more sophisticated triggers beyond the basic yet powerful patch trigger, we conduct experiments using Instagram filter triggers [28]. A demonstration of the

filter effects is presented in Fig. 7, where the Gotham filter introduces blurring and a gray tone, while the Lomo filter creates a vignette effect. As shown in Tab. 5, ETF-FT remains effective even against this more subtle type of trigger.

4.3.3. Adaptive Attack

Consider a scenario where the adversary is aware that trojan attacks undermine the phenomenon of Neural Collapse. Thus, they train the model with the final layer’s weights fixed as an ETF, effectively replicating the conditions under which Neural Collapse occurs perfectly. ETF-FT demonstrates robust performance even in the face of adaptive attacks. As evidenced in Tab. 6, the ASR is only 90.65, which is lower than the ASR observed in other similar settings. This supports our observation that trojan attacks are incompatible with the Neural Collapse mechanism. Notably, ETF-FT not only removes the trojans but also enhances the model’s Accuracy.

	ACC	ASR
Original (W fixed as ETF)	87.68	90.65
ETF-FT (5% clean data)	91.48 ± 0.18	2.56 ± 0.67
ETF-FT (1% clean data)	89.91 ± 0.3	4.61 ± 4.22

Table 6. **Adaptive Attack:** Performance of ETF-FT on trojaned model trained with **final layer fixed as ETF**. Results are reported on 10% Badnets trojaned CIFAR-10 using PreAct-ResNet18, averaged over 10 random trials (mean \pm std).

4.3.4. Cleansing Without Overtraining

Neural Collapse occurs most strongly in models trained well past zero training error. In line with this, our other experiments used models trained for 350 epochs, despite reaching zero training error at approximately 120 epochs. However, in practical scenarios, models may not always be overtrained. To examine ETF-FT’s reliance on model overtraining we also test it on models trained only until the training error reaches zero. As shown in Tab. 7, ETF-FT maintains strong performance in this case, achieving comparable results to its performance on overtrained models.

	ACC	ASR
Original	90.66	94.78
ETF-FT (5% clean data)	91.3 ± 0.1	0.86 ± 0.23
ETF-FT (1% clean data)	89.54 ± 0.31	0.72 ± 0.23

Table 7. **No Overtraining:** Performance of ETF-FT on trojaned model only trained for **120 epochs**. Results are reported on 10% Badnets trojaned CIFAR-10 using PreAct-ResNet18, averaged over 10 random trials (mean \pm std).

5. Conclusion

In this paper, we explore how the asymmetry induced by a trojan trigger in a neural network disrupts the phenomenon of Neural Collapse. We provide experimental evidence showing that trojan attacks significantly weaken NC based on standard metrics. Leveraging these insights, we propose a novel method for trojan cleansing: by fixing the network’s final layer to a simplex ETF—an ideal structure predicted by NC—and fine-tuning on a small amount of clean data. Our results show that this approach effectively removes the trojan trigger while maintaining the network’s accuracy on clean test data without requiring knowledge of the trigger type, the target class, or access to the original training data. Moreover, our method can be applied to any standard architecture with no modification.

5.1. Future Work

This work suggests a variety of interesting future directions. Given the significant experimental evidence of the connection between trojans and Neural Collapse, developing a theoretical framework as well as building a trojan detection method are important areas of future work.

In this work, we used a randomly generated ETF as the starting point in our cleansing strategy; characterizing the impact of the initial ETF selection as well as optimizing this are other interesting areas of investigation.

This paper focuses on image classification, but trojans have also been proven effective in other domains such as language and audio. Extending our analysis and cleansing mechanism to these domains is an interesting direction for future work.



Figure 7. Instagram filter effect: Original (Top), Gotham (Middle), Lomo (Bottom)

Method	Gotham		Lomo	
	ACC	ASR	ACC	ASR
Original	93.66	100	93.21	100
FT	89.84 ± 0.35	24.5 ± 21.58	89.92 ± 0.22	3.6 ± 2.11
NCleanse[29]	84.54 ± 6.05	70.49 ± 28.77	83.1 ± 5.18	22.68 ± 38.73
NAD[17]	29.48 ± 2.61	4.14 ± 4.03	29.52 ± 2.48	0.0 ± 0.0
NPD[37]	87.21 ± 2.53	3.87 ± 5.29	87.68 ± 3.62	20.82 ± 18.39
FT-SAM[36]	85.94 ± 1.42	10.59 ± 12.85	86.93 ± 1.22	1.84 ± 1.03
I-BAU[33]	90.34 ± 0.86	39.12 ± 27.04	89.86 ± 1.56	8.84 ± 5.58
ETF-FT(ours)	85.4 ± 0.54	14.9 ± 20.7	85.33 ± 0.52	2.28 ± 1.29

Table 5. Performance comparison of cleansing algorithms on Trojaned models trained with 10% poisoned data using the BadNets attack, where the trigger is the **Gotham and Lomo Instagram filters**. Cleansing is performed with 5% clean data. Results are reported on 10% Badnets trojaned CIFAR-10 using PreAct-ResNet18, averaged over 10 random trials (mean ± std).

References

- [1] Dosovitskiy Alexey. An image is worth 16x16 words: Transformers for image recognition at scale. *arXiv preprint arXiv:2010.11929*, 2020. 6, 7
- [2] Nathalie Baracaldo, Bryant Chen, Heiko Ludwig, and Jaehoon Amir Safavi. Mitigating poisoning attacks on machine learning models: A data provenance based approach. In *Proceedings of the 10th ACM workshop on artificial intelligence and security*, pages 103–110, 2017. 3
- [3] Bryant Chen, Wilka Carvalho, Nathalie Baracaldo, Heiko Ludwig, Benjamin Edwards, Taesung Lee, Ian Molloy, and Biplav Srivastava. Detecting backdoor attacks on deep neural networks by activation clustering. *arXiv preprint arXiv:1811.03728*, 2018. 3
- [4] Huili Chen, Cheng Fu, Jishen Zhao, and Farinaz Koushanfar. Deepinspect: A black-box trojan detection and mitigation framework for deep neural networks. pages 4658–4664, 2019. 3
- [5] Xinyun Chen, Chang Liu, Bo Li, Kimberly Lu, and Dawn Song. Targeted backdoor attacks on deep learning systems using data poisoning. *arXiv preprint arXiv:1712.05526*, 2017. 2
- [6] Xiaoyi Chen, Ahmed Salem, Dingfan Chen, Michael Backes, Shiqing Ma, Qingni Shen, Zhonghai Wu, and Yang Zhang. Badnl: Backdoor attacks against nlp models with semantic-preserving improvements. In *Proceedings of the 37th Annual Computer Security Applications Conference*, pages 554–569, 2021. 2
- [7] Jiazhu Dai, Chuanshuai Chen, and Yufeng Li. A backdoor attack against lstm-based text classification systems. *IEEE Access*, 7:138872–138878, 2019. 2
- [8] Khoa Doan, Yingjie Lao, Weijie Zhao, and Ping Li. Lira: Learnable, imperceptible and robust backdoor attacks. In *Proceedings of the IEEE/CVF international conference on computer vision*, pages 11966–11976, 2021. 2
- [9] Greg Fields, Mohammad Samragh, Mojan Javaheripi, Farinaz Koushanfar, and Tara Javidi. Trojan signatures in dnn weights. In *Proceedings of the IEEE/CVF International Conference on Computer Vision*, pages 12–20, 2021. 3
- [10] Tianyu Gu, Kang Liu, Brendan Dolan-Gavitt, and Siddharth Garg. Badnets: Evaluating backdooring attacks on deep neural networks. *IEEE Access*, 7:47230–47244, 2019. 1, 2, 6
- [11] Li Guo, Keith Ross, Zifan Zhao, George Andriopoulos, Shuyang Ling, Yufeng Xu, and Zixuan Dong. Cross entropy versus label smoothing: A neural collapse perspective. *arXiv preprint arXiv:2402.03979*, 2024. 3
- [12] XY Han, Vardan Papyan, and David L Donoho. Neural collapse under mse loss: Proximity to and dynamics on the central path. *arXiv preprint arXiv:2106.02073*, 2021. 3
- [13] Kaiming He, Xiangyu Zhang, Shaoqing Ren, and Jian Sun. Identity mappings in deep residual networks. In *Computer Vision—ECCV 2016: 14th European Conference, Amsterdam, The Netherlands, October 11–14, 2016, Proceedings, Part IV 14*, pages 630–645. Springer, 2016. 6, 7
- [14] Wanli Hong and Shuyang Ling. Neural collapse for unconstrained feature model under cross-entropy loss with imbalanced data. *Journal of Machine Learning Research*, 25(192): 1–48, 2024. 3
- [15] Mojan Javaheripi, Mohammad Samragh, Gregory Fields, Tara Javidi, and Farinaz Koushanfar. Cleann: accelerated trojan shield for embedded neural networks. In *Proceedings of the 39th International Conference on Computer-Aided Design*, page 1–9. ACM, 2020. 3
- [16] Vignesh Kothapalli. Neural collapse: A review on modelling principles and generalization. *arXiv preprint arXiv:2206.04041*, 2022. 3
- [17] Yige Li, Xixiang Lyu, Nodens Koren, Lingjuan Lyu, Bo Li, and Xingjun Ma. Neural attention distillation: Erasing backdoor triggers from deep neural networks, 2021. 2, 6, 7, 9, 1
- [18] Yuntao Liu, Yang Xie, and Ankur Srivastava. Neural trojans. In *2017 IEEE International Conference on Computer Design (ICCD)*, pages 45–48, 2017. 3
- [19] Yingqi Liu, Shiqing Ma, Yousra Aafer, Wen-Chuan Lee, Juan Zhai, Weihang Wang, and Xiangyu Zhang. Trojaning attack on neural networks. In *25th Annual Network And Distributed System Security Symposium (NDSS 2018)*. Internet Soc, 2018. 2, 6, 7

- [20] Yunfei Liu, Xingjun Ma, James Bailey, and Feng Lu. Reflection backdoor: A natural backdoor attack on deep neural networks. In *Computer Vision—ECCV 2020: 16th European Conference, Glasgow, UK, August 23–28, 2020, Proceedings, Part X 16*, pages 182–199. Springer, 2020. [2](#)
- [21] Wanlun Ma, Derui Wang, Ruoxi Sun, Minhui Xue, Sheng Wen, and Yang Xiang. The” beatrix”resurrections: Robust backdoor detection via gram matrices. *arXiv preprint arXiv:2209.11715*, 2022. [3](#)
- [22] Preetum Nakkiran, Gal Kaplun, Yamini Bansal, Tristan Yang, Boaz Barak, and Ilya Sutskever. Deep double descent: Where bigger models and more data hurt. *Journal of Statistical Mechanics: Theory and Experiment*, 2021(12):124003, 2021. [3](#)
- [23] Anh Nguyen and Anh Tran. Wanet—imperceptible warping-based backdoor attack. *arXiv preprint arXiv:2102.10369*, 2021. [2](#)
- [24] Vardan Papyan, X. Y. Han, and David L. Donoho. Prevalence of neural collapse during the terminal phase of deep learning training. *Proceedings of the National Academy of Sciences*, 117(40):24652–24663, 2020. [1](#), [2](#), [3](#)
- [25] Aniruddha Saha, Akshayvarun Subramanya, and Hamed Pirsiavash. Hidden trigger backdoor attacks, 2019. [1](#)
- [26] Shiqi Shen, Shruti Tople, and Prateek Saxena. Auror: Defending against poisoning attacks in collaborative deep learning systems. In *Proceedings of the 32nd annual conference on computer security applications*, pages 508–519, 2016. [3](#)
- [27] Ruixiang Tang, Mengnan Du, Ninghao Liu, Fan Yang, and Xia Hu. An embarrassingly simple approach for trojan attack in deep neural networks. In *Proceedings of the 26th ACM SIGKDD international conference on knowledge discovery & data mining*, pages 218–228, 2020. [1](#)
- [28] TrojAI Project. Trojai instagram transforms module, 2025. Accessed: 2025-03-01. [7](#)
- [29] Bolun Wang, Yuanshun Yao, Shawn Shan, Huiying Li, Bimal Viswanath, Haitao Zheng, and Ben Y. Zhao. Neural cleanse: Identifying and mitigating backdoor attacks in neural networks. In *2019 IEEE Symposium on Security and Privacy (SP)*, pages 707–723, 2019. [2](#), [6](#), [7](#), [9](#), [1](#)
- [30] Baoyuan Wu, Hongrui Chen, Mingda Zhang, Zihao Zhu, Shaokui Wei, Danni Yuan, and Chao Shen. Backdoor-bench: A comprehensive benchmark of backdoor learning. *Advances in Neural Information Processing Systems*, 35: 10546–10559, 2022. [3](#), [6](#)
- [31] Jun Xia, Ting Wang, Jiepin Ding, Xian Wei, and Mingsong Chen. Eliminating backdoor triggers for deep neural networks using attention relation graph distillation, 2022. [2](#)
- [32] Jianbin Ye, Xiaoyuan Liu, Zheng You, Guowei Li, and Bo Liu. Drinet: Dynamic backdoor attack against automatic speech recognition models. *Applied Sciences*, 12(12), 2022. [2](#)
- [33] Yi Zeng, Si Chen, Won Park, Z Morley Mao, Ming Jin, and Ruoxi Jia. Adversarial unlearning of backdoors via implicit hypergradient. *arXiv preprint arXiv:2110.03735*, 2021. [3](#), [6](#), [7](#), [9](#), [1](#)
- [34] Jiayao Zhang, Hua Wang, and Weijie Su. Imitating deep learning dynamics via locally elastic stochastic differential equations. *Advances in Neural Information Processing Systems*, 34:6392–6403, 2021. [3](#)
- [35] Songzhu Zheng, Yikai Zhang, Hubert Wagner, Mayank Goswami, and Chao Chen. Topological detection of trojaned neural networks. *Advances in Neural Information Processing Systems*, 34:17258–17272, 2021. [2](#)
- [36] Mingli Zhu, Shaokui Wei, Li Shen, Yanbo Fan, and Baoyuan Wu. Enhancing fine-tuning based backdoor defense with sharpness-aware minimization. In *Proceedings of the IEEE/CVF International Conference on Computer Vision*, pages 4466–4477, 2023. [3](#), [6](#), [7](#), [9](#), [1](#)
- [37] Mingli Zhu, Shaokui Wei, Hongyuan Zha, and Baoyuan Wu. Neural polarizer: A lightweight and effective backdoor defense via purifying poisoned features. *Advances in Neural Information Processing Systems*, 36, 2024. [3](#), [6](#), [7](#), [9](#), [1](#)
- [38] Zhihui Zhu, Tianyu Ding, Jinxin Zhou, Xiao Li, Chong You, Jeremias Sulam, and Qing Qu. A geometric analysis of neural collapse with unconstrained features. *Advances in Neural Information Processing Systems*, 34:29820–29834, 2021. [3](#)

Trojan Cleansing with Neural Collapse

Supplementary Material

A. More Cleansing Results

Method	ACC	ASR
Original	88.95	95.06
FT	86.01 ± 1.59	22.95 ± 19.81
NCleanse[29]	88.43 ± 0.29	1.19 ± 0.27
NAD[17]	83.41 ± 1.87	3.17 ± 0.72
NPD[37]	83.10 ± 3.64	5.97 ± 4.59
FT-SAM[36]	87.20 ± 0.54	7.17 ± 3.69
I-BAU[33]	85.97 ± 1.43	49.55 ± 12.15
ETF-FT(ours)	88.16 ± 0.56	7.18 ± 2.06

Table 8. **Data Imbalance:** Comparison of cleansing algorithms with **1%** imbalanced clean training data on BadNet trojaned ResNet models(%). Results are averaged over 5 random trials with mean \pm std.